

## Photoelectromagnetic Effect in Tellurium\*

TAKEMARO SAKURAI AND MAREO ISHIGAME

*The Research Institute for Scientific Measurements, Tohoku University, Sendai, Japan*

(Received 20 April 1964)

The photoelectromagnetic (PEM) effect in tellurium was observed by using highly purified single crystals. The observed variation in the PEM voltage with magnetic field was linear to 3500 G in the chemically etched specimen, while in the specimen having an optical polish it was linear to 2500 G. The variation of the PEM voltage with illumination in the etched specimen was linear in the observed range, from  $10^{14}$  to  $10^{16}$  quanta/cm<sup>2</sup> sec. From the temperature dependence of the PEM voltage and that of the photoconductive voltage, it was found that the lifetime of the electrons was different from that of the holes, indicating that trapping of electrons took place at low temperatures. From the spectral dependence of the PEM effect, it was found that the effect occurred only in the main absorption band and that the half-value of the maximum sensitivity occurred at different wavelengths for light polarized parallel and perpendicular to the *c* axis.

### I. INTRODUCTION

THE photoelectromagnetic (PEM) effect occurs when a slab of semiconductor, illuminated on one of its surfaces, is placed in a magnetic field perpendicular to the direction of illumination. A voltage appears in the third perpendicular direction. This effect has been observed in several semiconductors. Carvalho<sup>1</sup> measured the PEM voltage of tellurium in various magnetic fields, but little further investigation seems to have been undertaken concerning the behavior of the effect.

In the present research, the dependence of the PEM effect on magnetic field, illumination, temperature, and wavelength was investigated. At the same time, the temperature dependence of the photoconductive effect was observed, because comparison of its temperature dependence with that of the PEM effect gives some knowledge of the mechanism of recombination of the photocarriers.

### II. SPECIMENS AND EXPERIMENTAL ARRANGEMENTS

The specimens used were cut by a diamond cutter from very pure single crystals of tellurium into a rectangular shape, 1.0 cm in length and 1 mm×4 mm in cross section. Two kinds of specimens were prepared;  $T_1$  was ground and polished by metallographic and optical techniques, and  $T_2$  was etched with a  $\text{HNO}_3 + \text{H}_2\text{O}$  solution after receiving the treatments described above. The electrical contact to the specimen was made by welding Pt wire by means of a condensed discharge. The surface illuminated was the plane (10 $\bar{1}$ 0).

The optical arrangements used were nearly the same as those used in the observation of the PEM effect in Ge.<sup>2</sup> As they have been reported in detail previously, only a brief description will be given here. The light from a Globar was chopped at the rate of 10 cps and was introduced into the entrance slit of a monochromator provided with a lithium fluoride prism. The

monochromatic beam from the exit slit was divided into two directions by beam splitter. One beam was focused on a thermojunction, while the other beam was focused on a specimen in a cryostat placed between the poles of an electromagnet. In order to illuminate the specimen with the light of equal intensity but different wavelengths, the slits of the monochromator were adjusted so that the thermojunction always gave equal output. For the absolute measurement of the intensity of illumination, a radiometer specially fabricated for this purpose was used. As it has already been described in detail,<sup>2</sup> no further description will be given here. The PEM voltage was measured by an amplifier tuned to 10 cps. The small voltage induced by the photo-voltaic effect was eliminated by comparing the values for two opposite directions of the magnetic field.

### III. RESULTS OBTAINED AND DISCUSSION

#### 1. Variation of the PEM Effect with Magnetic Field

Figure 1 is the observed PEM voltage of the specimens  $T_1$  and  $T_2$  at room temperature plotted against the applied magnetic field. It is seen in this figure that

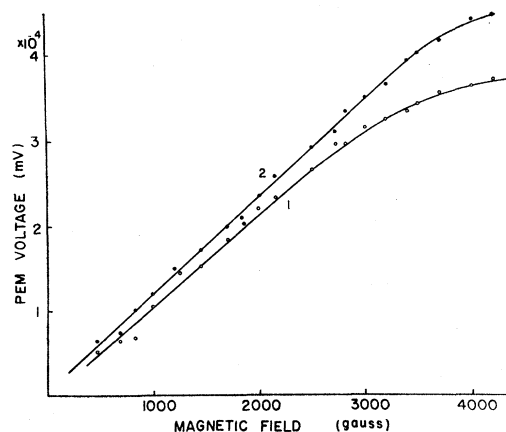


FIG. 1. Variation of PEM voltage with magnetic field.  $I = 3 \times 10^{15}$  quanta/cm<sup>2</sup> sec, and  $T = 300^\circ\text{K}$ . Curves 1 and 2 are for the specimens  $T_1$  and  $T_2$ .

\* Supported in part by the Grant in Aid of Scientific Research by the Ministry of Education.

<sup>1</sup> A. A. P. de Carvalho, *Compt. Rend.* **242**, 745 (1956).

<sup>2</sup> M. Ishigame, *Japan. J. Appl. Phys.* **3**, 250 (1964).

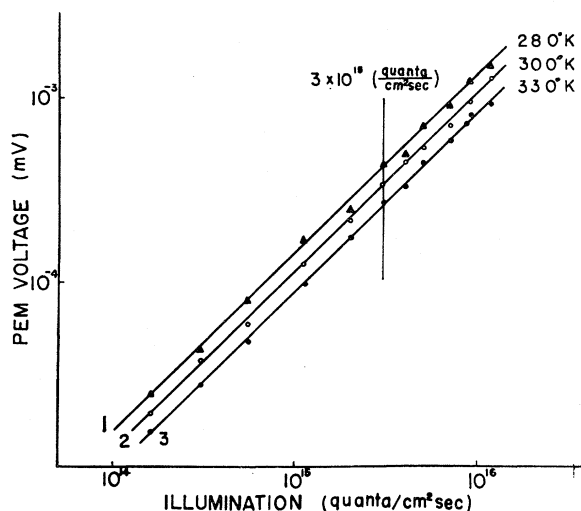


FIG. 2. PEM voltage versus illumination at various temperatures.  $B = 3000$  G.

the variation of the PEM voltage with magnetic field is linear to about 2500 G in the specimen  $T_1$ , while in the specimen  $T_2$  it was linear to about 3000 G. A departure from the linearity appears in stronger fields. Carvalho observed the variation in the PEM effect in tellurium with magnetic field and found that saturation was reached in a field of about 20 000 G. The results obtained in our observed range of magnetic field agree with his results.

The theory of the PEM effect is simple for weak magnetic fields where linearity exists between the PEM voltage and the magnetic field. Therefore, in the sub-

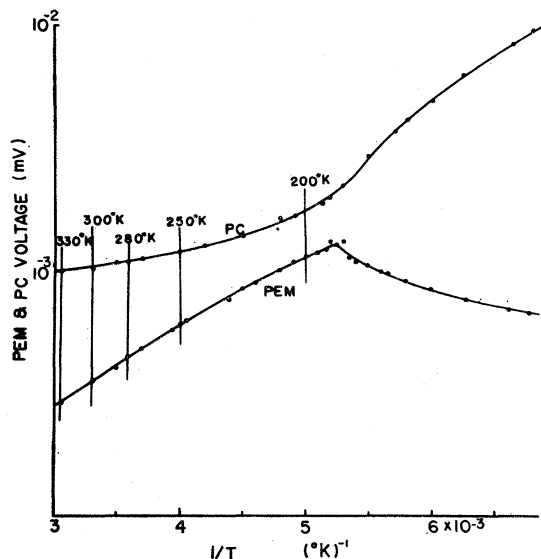


FIG. 3. PEM voltage and photoconductive voltage as a function of reciprocal temperature.  $I = 3 \times 10^{15}$  quanta/cm<sup>2</sup> sec, and  $B = 3000$  G.

sequent experiment, the magnetic field was less than 3000 G.

### 2. Variation of the PEM Effect with Illumination

The variation of the PEM effect with illumination was measured by using the specimen  $T_2$ . The radiation used was  $2.5 \mu$  in wavelength and the magnetic field applied was 3000 G.

Figure 2 is the measured PEM open circuit voltage plotted against the intensity of illumination in terms of quanta/cm<sup>2</sup> sec on a logarithmic scale. In this figure, the curves 1, 2, and 3 are the values of the PEM voltage obtained at 280, 300, and 330°K, respectively. These curves are straight and make an angle of 45° with the axis of abscissa, which indicates that the PEM voltages

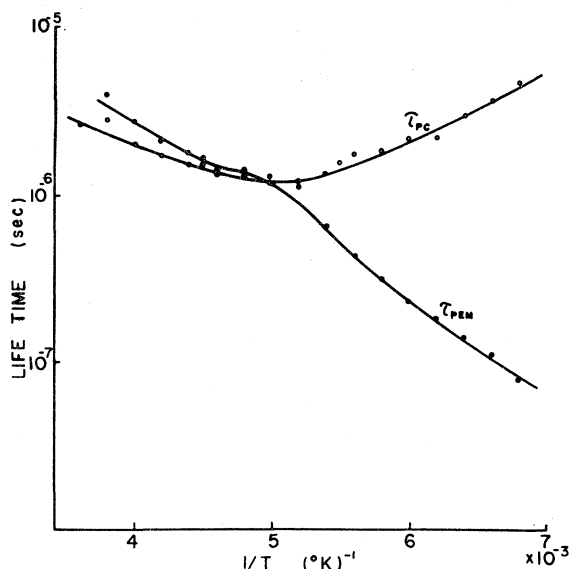


FIG. 4. Temperature dependence of  $\tau_{PEM}$  and  $\tau_{PC}$ .

vary linearly with the light intensity. Moss, Pincherle, and Woodward<sup>3</sup> observed at room temperature the variation in the PEM open circuit voltage in germanium with an illumination as large as  $10^{18}$  quanta/cm<sup>2</sup> sec, and found that saturation was reached for strong illumination. In tellurium, however, saturation is not reached with an illumination of  $10^{16}$  quanta/cm<sup>2</sup> sec.

### 3. Variation in the PEM and in the Photoconductive Effect with Temperature

The variation in the PEM and photoconductive voltages with temperature were observed in the same specimen. The PEM voltage was measured with an illumination of  $3 \times 10^{15}$  quanta/cm<sup>2</sup> sec and with a magnetic field of 3000 G. The photoconductive voltage

<sup>3</sup> T. S. Moss, L. Pincherle, and A. M. Woodward, Proc. Phys. Soc. (London) **B66**, 743 (1953).

was measured with an illumination of  $3 \times 10^{15}$  quanta/cm<sup>2</sup> sec and with an electric field of 0.02 V/cm.

In Fig. 3, the observed PEM voltage and photoconductive voltage are represented as a function of the reciprocal of the temperature expressed in  $^{\circ}\text{K}^{-1}$ . It is seen in this figure that the PEM voltage increases to about 200 $^{\circ}\text{K}$  and then decreases as the temperature decreases, while the photoconductive voltage increases as the temperature decreases. The temperature dependence of the PEM effect and that of the photoconductive effect are caused by the variation in mobility, charge carrier concentration, and lifetime with temperature. As the variations in mobility and charge carrier concentration with temperature are determined by measuring the electrical conductivity and the Hall constant as a function of temperature, it is possible to give the variation in lifetime in both effects. Using the values of the curves in Fig. 3, the lifetimes  $\tau_{\text{PEM}}$  and  $\tau_{\text{PC}}$  can be determined at various temperatures, as shown in Fig. 4. It is seen in this figure that at temperatures above 200 $^{\circ}\text{K}$ , the values of  $\tau_{\text{PEM}}$  are in good accord with those of  $\tau_{\text{PC}}$ . This result shows that the lifetime of electrons and holes are equal in this temperature range. On the other hand, at temperatures below 200 $^{\circ}\text{K}$ ,  $\tau_{\text{PEM}}$  decreases while  $\tau_{\text{PC}}$  increases with temperature.

On the basis of Zitter's theory,<sup>4</sup>  $\tau_{\text{PEM}}$  and  $\tau_{\text{PC}}$  are expressed by the following equations:

$$\tau_{\text{PEM}} = \frac{\tau_n + c\tau_p}{1+c}, \quad \tau_{\text{PC}} = \frac{\tau_n + (\tau_p/b)}{1+(1/b)}, \quad (1)$$

where  $b$  is  $(\mu_n/\mu_p)$ , electron mobility/hole mobility,  $c$  is

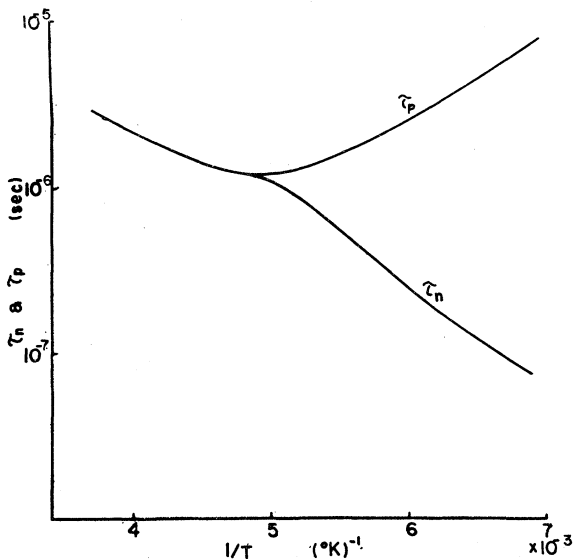


FIG. 5. Temperature dependence of electron and hole lifetimes.

<sup>4</sup> R. N. Zitter, Phys. Rev. 112, 852 (1958).

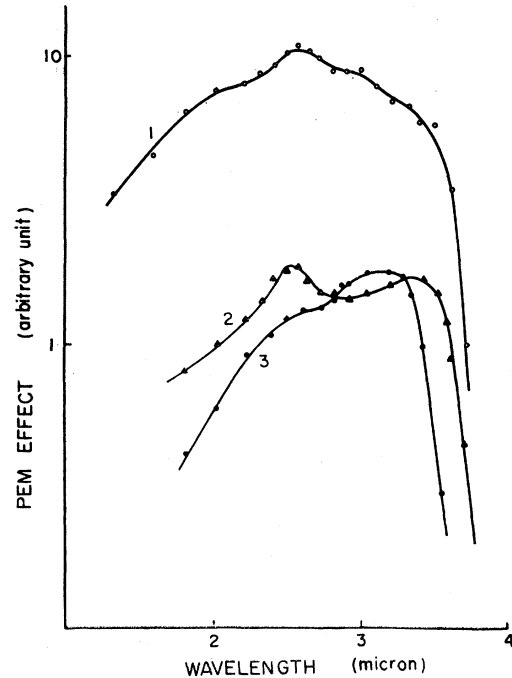


FIG. 6. Spectral dependence of PEM effect. Curve 1 is for the unpolarized light. Curves 2 and 3 are for light polarized perpendicular and parallel to  $c$  axis, respectively.

$n_0/p_0$ ,  $n_0$  is the equilibrium concentration of electrons,  $p_0$  is the equilibrium concentration of holes,  $\tau_n$  is the electron lifetime,  $\tau_p$  is the hole lifetime. The values of  $b$  and  $c$  were determined by measuring the electrical conductivity and the Hall constant as a function of temperature. The value of  $b$  obtained was 2.0 in the temperature range between 150 and 300 $^{\circ}\text{K}$ . The specimen used was extrinsic and  $p$  type at temperatures below 200 $^{\circ}\text{K}$ . In this region, it may be considered that  $c \approx 0$ . Hence, the lifetimes  $\tau_n$  and  $\tau_p$  can be determined by using the observed values of  $\tau_{\text{PEM}}$  and  $\tau_{\text{PC}}$ . In Fig. 5,  $\tau_n$  and  $\tau_p$  are plotted against the inverse of temperature. It will be seen in this figure that  $\tau_n$  and  $\tau_p$  are not equal below 200 $^{\circ}\text{K}$  and  $\tau_n$  decreases while  $\tau_p$  increases with temperature. Such a temperature dependence is interpreted as the result of the trapping of the electrons in this temperature range. It should be noted that the trapping effect in tellurium has been also observed by Blakemore *et al.*<sup>5</sup> by the photoconductive method.

#### 4. Spectral Dependence of the PEM Effect

The spectral sensitivity of the PEM effect was measured with a magnetic field of about 3000 G. Figure 6 illustrates the observed spectral distribution of the sensitivity of the PEM effect. Curve 1 in Fig. 6 shows that the quantum efficiency of the PEM effect

<sup>5</sup> J. S. Blakemore, J. D. Heaps, K. C. Nomura, and L. P. Beardsley, Phys. Rev. 117, 687 (1960).

increases slowly with wavelength, passes through a maximum, and falls rapidly at the longer wavelengths. The wavelength at which the sensitivity becomes half of the maximum value is  $3.8 \mu$ . This value corresponds to an energy of 0.33 eV which is in good agreement with the value obtained by measuring the absorption coefficient. Curves 2 and 3 are the quantum efficiency of the PEM effect for light polarized perpendicular and parallel to the  $c$  axis of the crystal. Comparing these

curves, it will be seen that the wavelength  $\lambda(\frac{1}{2})$  at which the sensitivity becomes a half of the maximum value is  $3.4 \mu$  in curve 3 and  $3.7 \mu$  in curve 2. The discrepancy between the two curves is interpreted as the result of the anisotropy of the crystal structure of tellurium. This interpretation is supported by observations of the absorption coefficient of tellurium.<sup>6</sup>

<sup>6</sup> J. J. Loferski, Phys. Rev. **93**, 707 (1954).

## Lattice Sum Evaluations of Ruby Spectral Parameters\*

J. O. ARTMAN AND JOHN C. MURPHY

*Applied Physics Laboratory, The Johns Hopkins University, Silver Spring, Maryland*

(Received 4 March 1964; revised manuscript received 15 April 1964)

This paper presents the results of an attempt to collate many of the known spectroscopic properties of ruby in the strong field coupling scheme within the framework of an ionic model. The Tanabe-Sugano theory extended to odd symmetry crystal fields is used in this analysis. The appropriate Madelung and higher order potentials are computed for both a point-ion and a point-dipolar lattice. The radius of convergence of these sums found with our procedure is much smaller than those reported by McClure and others. The lattice potentials derived from a particular model of the  $\text{Cr}^{3+}$  local environment give a reasonable fit to many of the measurable spectroscopic parameters. In addition to the conventional optical splittings, these include optical intensities, pressure and "electric field" effects. The interpretation of the  $\text{Cr}^{63}$  nuclear electric quadrupole moment is shown to be sensitive to the details of the  $\text{Cr}^{3+}$  environment. Some results are given for other ions and also for  $\text{Al}^{3+}$  in corundum.

### INTRODUCTION

THE general procedure that will be followed in this paper is to assume the so-called crystal-field theory in its most general form. Here the form of the tensor operators is determined by the symmetry of the site under consideration and the tensor coefficients are determined from experiment. It follows that within the framework of the theory relations exist between quite diverse experimental parameters which depend only on the symmetry of the site under consideration. Subsequently, an "ionic" model for the interactions in the corundum lattice will be introduced which will be used to evaluate many of these potential coefficients explicitly by the method of lattice sums. This approximation to the actual interactions in a crystal clearly is quite crude in comparison to a complete molecular-orbital treatment. However, carrying out this latter program leads to conceptual and computational difficulties. Those calculations which have actually been made to date required approximations whose validity is uncertain. Covalency effects have been introduced, for example, via a limited number of adjustable parameters such as the Koide-Pryce  $\epsilon$  or the ionization potential of the ions in the crystal; interactions with the rest of the lattice were ignored despite the long-range character of the

Coulomb interaction.<sup>1-3</sup> In such a situation the actual usefulness of the separate approximations probably depends on what experimental aspects of the problem are under consideration.

Recently, Sugano and Shulman<sup>4</sup> performed a complete molecular orbital calculation on the  $(\text{NiF}_6)^{4-}$  complex in  $\text{KMnF}_3$  neglecting the rest of the lattice and have obtained good agreement with experiment. If we leave aside some recent criticism<sup>4</sup> of their molecular orbital procedure, their calculations would indicate that a large degree of covalency is required for this structure. They justify the neglect of extracomplex interactions by showing that the potential field of the entire lattice outside of the complex under consideration evaluated at the nuclear position of each member of the complex is approximately constant. (The variation of this "reduced" Madelung potential evaluated at Ni and F sites is 0.26 eV.) The complex is thus immersed in a field of constant potential and to a first approximation

<sup>1</sup> S. Koide and M. H. L. Pryce, Phil. Mag. **3**, 607 (1958).

<sup>2</sup> S. Sugano and M. Peter, Phys. Rev. **122**, 381 (1961).

<sup>3</sup> L. L. Lohr, Jr., and W. N. Lipscomb, J. Chem. Phys. **38**, 1607 (1963).

<sup>4</sup> R. G. Shulman and S. Sugano, Phys. Rev. **130**, 506 (1963); K. Knox, R. G. Shulman, and S. Sugano, Phys. Rev. **130**, 512 (1963); S. Sugano and R. G. Shulman, Phys. Rev. **130**, 517 (1963). But see a recent criticism by R. E. Watson and A. J. Freeman, Phys. Rev. **134**, A1526 (1964) of the molecular orbital treatment employed in this work.

\* This work supported by the Bureau of Naval Weapons, U. S. Department of the Navy, under Contract NOW 62-0604-c.